Long-reach cost-effective 100 Gbit/s CO-OFDM-MDM-based inter-satellite optical wireless communication (IsOWC) system

KARAMJEET SINGH[a,d], MEHTAB SINGH[b,c,*], JYOTEESH MALHOTRA[b], AMIT GROVER[d]
*a*Department of Electronics and Communication Engineering, IKG-PTU, Kapurthala, India
*b*Department of Engineering and Technology, Guru Nanak Dev University, Regional Campus, Jalandhar, India
*c*Department of Electronics and Communication Engineering, SIET, Amritsar (IKG-PTU, Kapurthala), India
*d*Department of Electronics and Communication Engineering, Shaheed Bhagat Singh State University, Ferozepur, India

Inter-satellite links are crucial for covering the entire globe for information transmission. Traditional space communication systems are based on microwave links, which have high deployment and maintenance cost and high latency. Recently, the application of laser-based optical wireless communication links for inter-satellite applications has gained significant attention due to its many advantages including low deployment and maintenance cost, high modulation bandwidth, secure transmission, low latency networks, and high-speed transmission. In previous works reported on inter-satellite optical wireless communication (IsOWC) links, single-channel links employing conventional modulation formats are demonstrated. Future space technology demands inter-satellite links that permit high-speed information transmission between two or more satellites. In this work, to enhance the spectral-efficiency and transmission speed of IsOWC systems, mode division multiplexing technique is incorporated. Further, to transmit high-speed data without inter-symbol interference, orthogonal frequency division multiplexing with coherent detection is employed. Distinct Hermite Gaussian spatial modes are used to transport two independent 50 Gbit/s information signals at 20500 km. Also, the link performance is investigated for different modulation schemes and operating wavelengths. Further, the impact of space turbulence, including transmitter and receiver pointing errors on the received signal quality is analyzed. We also discuss a square root device-based detection for non-linearity compensation at the receiver for improved transmission range.

1. Introduction

The exponentially increasing internet services subscribers in the last few years has resulted in an increased demand for high channel capacity networks. As a result, an evolution in high channel capacity optical wireless links for terrestrial networks and space applications is witnessed. Laser technology-based data transmission is an effective solution to realize high data speed links between satellites orbiting in outer space. In the last few decades, inter-satellite optical wireless communication (IsOWC) technology has garnered substantial influence because of its inherit advantages like small beam size, high data rate and low power transmission, immunity to radio frequency and electromagnetic interference, and low cost of deployment [1, 2]. The European Space Agency demonstrated the first laser-based inter-satellite transmission link where high-definition images at 50 Mbit/s data speed were exchanges between SPOT-4 and ARTEMIS [3]. IsOWC links transmit the information through outer space where the atmospheric attenuation losses are absent. Therefore, the signal attenuation loss in IsOWC links is considered to be 0 dB/km [4]. Despite the merits, the performance of long-haul IsOWC links is degraded due to pointing errors

resulting from satellite platform vibrations, electronic equipment disturbances, and background noise radiations, which can result in total link failure [5-7]. The choice of modulation scheme and operating wavelength is considered vital while designing an IsOWC link to achieve maximum transmission distance and information transmission rate.

B. Patnaik et al. in [8] report the performance investigation of an IsOWC transmission link using quadrature phase shift keyed (QPSK) modulation. The transmission of 400 Gbit/s, 160 Gbit/s, and 100 Gbit/s QPSK information over 4767 km, 7542 km, and 9532 km IsOWC link distance respectively with faithful performance is reported. The simulative analysis of 10 Gbit/s return-to-zero differential phase shift keyed (RZ-DPSK) signal-based IsOWC link at 6000 km with 33%, 50%, and 67% duty cycle has been reported by G. Kumari et al. in [9]. The implementation of dynamic beam waist adjustment at the transmitter section to compensate for pointing errors in an IsOWC transmission link is discussed by T. Song et al. in [10]. A. Alipour et al. in [11] compared carrier-suppressed return-to-zero (CSRZ), duo-binary return-to-zero (DRZ), and modified duo-binary return-to-zero (MDRZ) modulation schemes in an IsOWC link employing 32-channnel wavelength division

multiplexed (WDM) system. 10 Gbit/s, 20 Gbit/s, and 40 Gbit/s information is transmitted at 250 km with good signal reception. MDRZ modulation scheme reported the best Quality Factor and bit error rate (BER) performance. R. Kaur et al. in [12] report a high data rate IsOWC link employing 64-channel WDM system with different modulation schemes. The results demonstrate that at 40 Gbit/s data rate, the differential phase shift keyed (DPSK) scheme performs the best followed by chirped return-to-zero and alternate mark inversion schemes. The performance of subcarrier multiplexing in a 7.2 Gbit/s IsOWC system is reported by S. Kumar et al. in [13]. A faithful transportation at 5000 km distance deploying the proposed link is reported. The modeling and performance analysis of 10 Gbit/s IsOWC link using orthogonal frequency division multiplexing (OFDM) and DPSK over 25000 km link range has been discussed by S. Chaudhary et al. in [14]. D. Amanor et al. in [15] have discussed the application of LED-based visible light communication in 2 Mbit/s IsOWC system at 0.5 km employing different intensity modulation and direct detection schemes. J. Padhy et al. in [16] realized a 40 Gbit/s-19100 km IsOWC link in the presence of space turbulence by employing DPSK and Manchester coding schemes. N. Kumar et al. in [17] report an improved performance of 2.5 Gbit/s-1000 km IsOWC link using non return-to-zero (NRZ) modulation and a square root device-based direct detection for compensating free space losses. The BER performance analysis of on-off keying, pulse position modulation (PPM), differential PPM, differential amplitude PPM, and pulse amplitude and position amplitude modulation in the scenario of inter-satellite link and earth-to-satellite uplink and downlink has been discussed by P. Gopal et al. in [18]. PPM scheme reported better performance under space turbulence. J. Padhy et al. in [19] report a 100 Gbit/s-15600 km IsOWC system employing hybrid WDM-OFDM techniques with advanced signal processing techniques for information retrieval. A radio over IsOWC system incorporating optical pre- and booster amplifier over 35000 km link distance is reported by K. Zong et al. in [20]. An IsOWC system with 7.63 Gbit/s-6000 km transmission employing hybrid space division multiplexing and polarization division multiplexing has been discussed by S. Pradhan et al. in [21]. K. Zong et al. in [22] report the modeling of an IsOWC link using dual-sideband suppressed carrier modulation and coherent homodyne detection for transmission of multi-band radio frequency signals. ANZ Rashid et al. in [23] discuss the analysis of a LEO-GEO IsOWC system at 20000 km employing higher order modulation schemes. The integration of optical code division multiplexed access and polarization multiplexing in an IsOWC system employing spectral amplitude coding is discussed by S. Chaudhary et al. in [24]. A 10 × 10 Gbit/s NRZ encoded data transportation at 10000 km is reported.

For realizing high channel bandwidth optical communication systems, coherent detection-OFDM (CO-OFDM) is considered as a promising and attractive technology, especially for long-haul high-speed optical transmission due to its many merits including high spectral efficiency, superior receiver sensitivity, availability of multiple modulation methods, long repeater spacing, flexible bandwidth allocation, robustness to non-linear effects and chromatic dispersion, and low cost transmission networks [25-27]. To meet the demands of exponentially rising internet-traffic, long-haul high-speed CO-OFDM-based optical communication links have been extensively studied in [28-30]. Further, to increase the number of channels and overall information capacity of the system, WDM-based IsOWC links have been studied in [31-34]. However in WDM-IsOWC systems, the cost and complexity of information transmission is increased due to the incorporation of multiple antennas and laser diodes [35].

Mode division multiplexed (MDM) systems simultaneously transmit multiple high data rate information streams over unique spatial laser modes of a single laser beam by exploiting the Eigenmode dimension [36, 37]. R. Gupta et al. in [38] demonstrate a comparative BER performance analysis of different amplifier configurations in a multi-input multi-output MDM-based optical fiber link over 100 km link range. C. Yi-Li et al. in [39] reported an experimental demonstration of a 320 Gbit/s MDM-based free space optics (FSO) link over 100 m link range using doublet lens scheme. The transmission of 9 independent channels using 9 distinct modes over 90 km multimode fiber link with acceptable BER has been demonstrated in [40]. R. Gupta et al. in [41] reported a short-reach 10 Tbit/s multimode fiber transmission by employing WDM and MDM systems. Y. Fazea et al. in [42] report the realization of Fiber-to-the-Home services by employing hybrid MDM and dense WDM systems in a passive optical network.

The works in [36-42] report the incorporation of MDM technique in optical fiber and FSO links. In optical fiber links, dispersion, polarization losses, signal power attenuation, and bending losses are the main factors degrading the performance of the transmission system. Similarly in FSO links, atmospheric weather related signal attenuation ranging from 0.14 dB/km under clear climate to 340 dB/km under dense fog along with turbulence induced scintillation effects are the most important factors which determine the system performance. Many research studies report the application of MDM systems in high capacity optical fiber and FSO links, but MDM in IsOWC links is still an underexplored area. The main performance deteriorating factors in IsOWC transmission are increasing range and pointing errors.

This work proposes a novel hybrid CO-OFDM-MDM-based IsOWC link and investigates its performance for increasing transmission range and pointing error losses. The motivation is to realize a spectral-efficient high capacity IsOWC transmission by employing hybrid CO-OFDM and MDM techniques. The spectral-efficiency is improved by incorporating MDM technique. High-speed long-reach information transmission with faithful BER performance is achieved using CO-OFDM technique. This paper is organized as follows- Section 2 presents a brief introduction to OFDM implementation in optical links followed by the proposed system design. Section 3

discusses the results and Section 4 concludes this research article.

2. System design of CO-OFDM-MDM-based IsOWC transmission system

OFDM is a broadband multi-carrier modulation technique capable of transmitting high data rate information over multiple parallel subcarriers, which are orthogonal to each other is the frequency domain. The implementation of OFDM in optical communication systems can achieve high data rate links with robustness against interference. The implementation of OFDM in optical communication systems such as in single mode optical fiber links [43-46], multimode optical fiber links [47-49], plastic optical fiber links [50], and optical wireless links [51] is discussed by different research groups. Fig. 1 illustrates the generalized schematic diagram of the OFDM transmitter and receiver for optical communication systems.
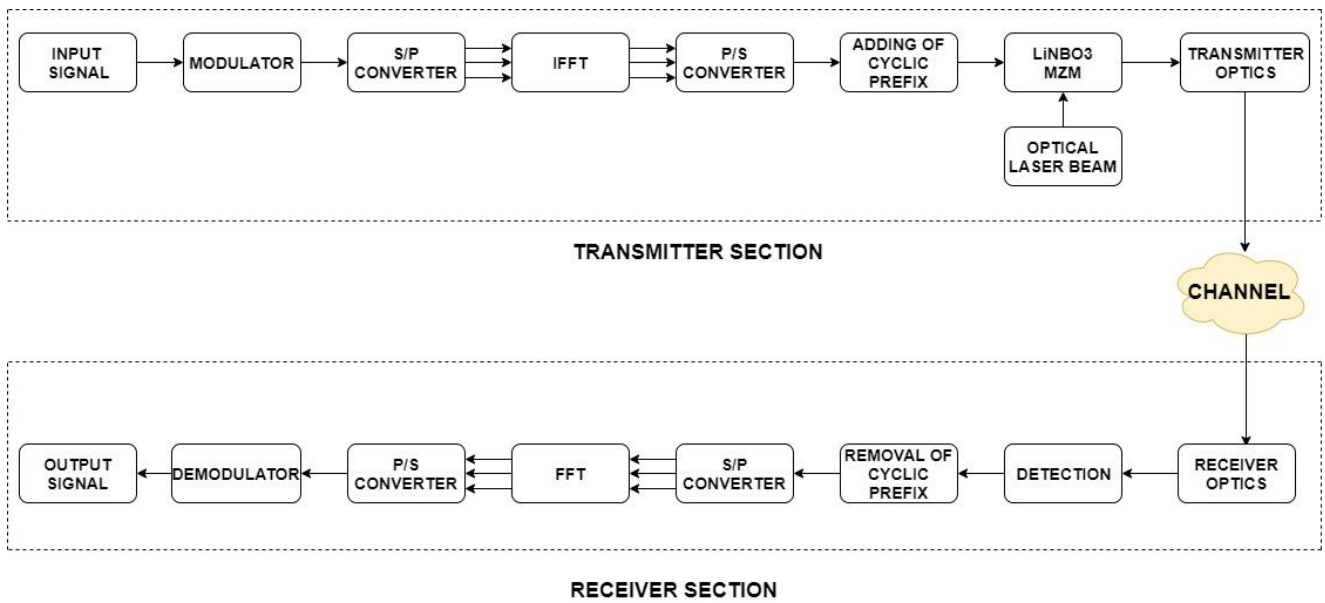

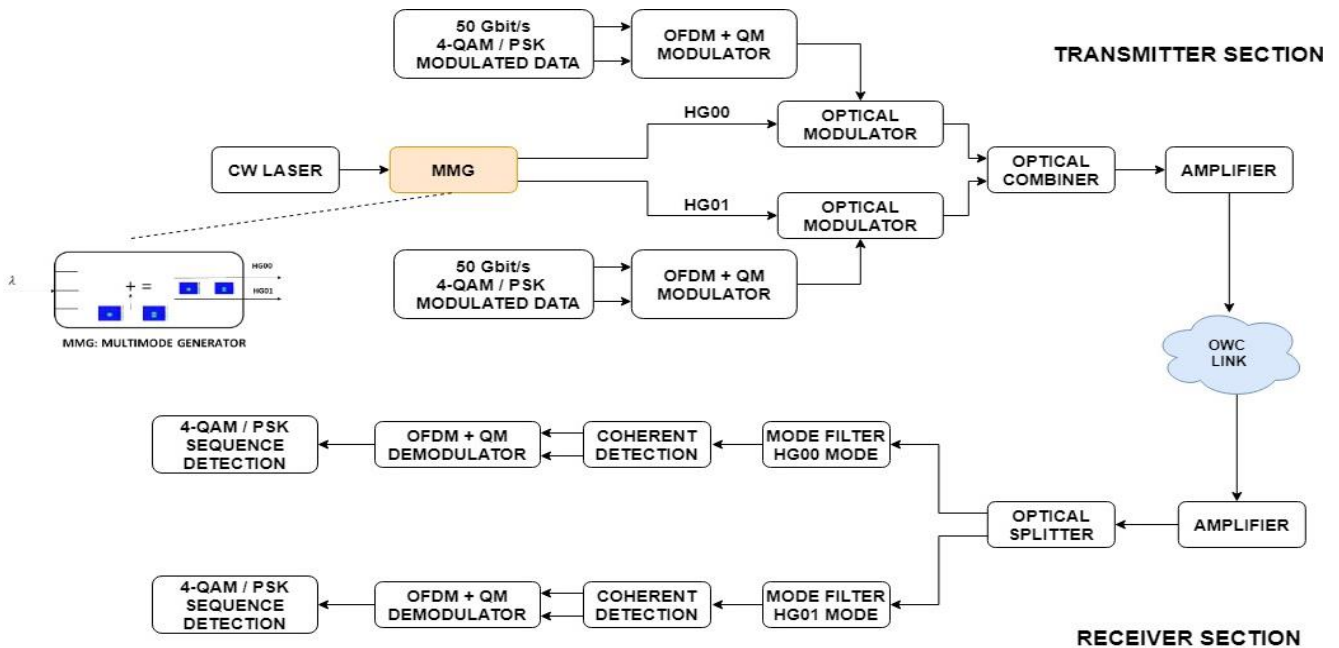Fig. 1. Generalized schematic diagram of OFDM in optical communication

Fig. 2. Proposed 100 Gbit/s CO-OFDM-MDM-based IsOWC transmission system (color online)

At the transmitter section, the input information signal is modulated which is then directed towards the Inverse Fast Fourier Transformation (IFFT) block through a serial-to-parallel (S/P) converter. In optical communication, quadrature amplitude modulation (QAM) is the most preferred modulation scheme [52]. The IFFT block has a complex vector input signal, $\mathbf{X} = [X_0 \, X_1 \, X_2 \, ... \, X_{N-1}]^T$ where N denotes the size of IFFT. Each element in the complex vector $\mathbf{X}$ denotes the information transported using the corresponding subcarrier. The IFFT block output is a complex vector $\mathbf{x} = [x_0 \, x_1 \, x_2 \, ... \, x_{N-1}]^T$ which can mathematically be described as [52]:

$$x_m = \frac{1}{\sqrt{N}} \sum_{k=0}^{N-1} X_k \exp\left(\frac{j2\pi km}{N}\right) \text{ for } 0 \leq m \leq N-1 \quad (1)$$

where k represents the symbol number. This parallel data is converted into serial data using a parallel-to-serial (P/S) converter. A cyclic prefix is added to this signal to eliminate interference. This information signal is then transmitted over an optical laser beam using lithium niobate (LiNBO3) mach-zehnder modulator (MZM) and transmitter optics. At the receiver section, the received information optical signal is detected using a photodiode. The cyclic prefix is removed from the information signal and then this signal is directed towards the Fast Fourier Transformation (FFT) block through a S/P converter. The input to the FFT block is a complex vector of the form $\mathbf{y} = [y_0 \, y_1 \, y_2 \, ... \, y_{N-1}]^T$ denoting sampled time domain information signal. At the output of the FFT block is a discrete frequency domain complex vector $\mathbf{Y} = [Y_0 \, Y_1 \, Y_2 \, ... \, Y_{N-1}]^T$ which can mathematically be described as [52]:

$$Y_k = \frac{1}{\sqrt{N}} \sum_{m=0}^{N-1} y_m \exp\left(\frac{-j2\pi km}{N}\right) \text{ for } 0 \leq k \leq N-1 \quad (2)$$

Here the channel is assumed to be noise free. This parallel data is then converted into serial data using a P/S converter. A demodulator unit retrieves the information bits. Fig. 2 illustrates the IsOWC transmission system design which is investigated using Optisystem software.

In this work, two Hermite Gaussian (HG) spatial modes simultaneously transmit 50 Gbit/s data streams. The intensity profiles of HG modes are given as [53]:

$$\psi_{l,n}(x,y) = H_l\left(\frac{\sqrt{2}x}{\omega_{0,x}}\right) \cdot \exp\left(-\frac{(x)^2}{\omega_{0x}^2}\right) \cdot \exp\left(j\frac{\pi(x)^2}{\lambda R_{0x}}\right) \times$$
$$H_n\left(\frac{\sqrt{2}y}{w_{0,y}}\right) \cdot \exp\left(-\frac{(y)^2}{w_{0y}^2}\right) \exp\left(j\frac{\pi(y)^2}{\lambda R_{0y}}\right) \quad (3)$$

where l represents modal dependency on the X-axis, n represents modal dependency on the Y-axis, R is the radius of spatial beam, H_l and H_n represent Hermite polynomials, and w_0 is spot size at beam waist. The authors in [54-58] discuss the physical behavior of the HG modes propagating in optical links. Here, HG spatial modes are excited using a continuous wave (CW) laser

with 30 dBm power and a multimode generator (MMG). Fig. 3 illustrates the intensity profiles of modes.
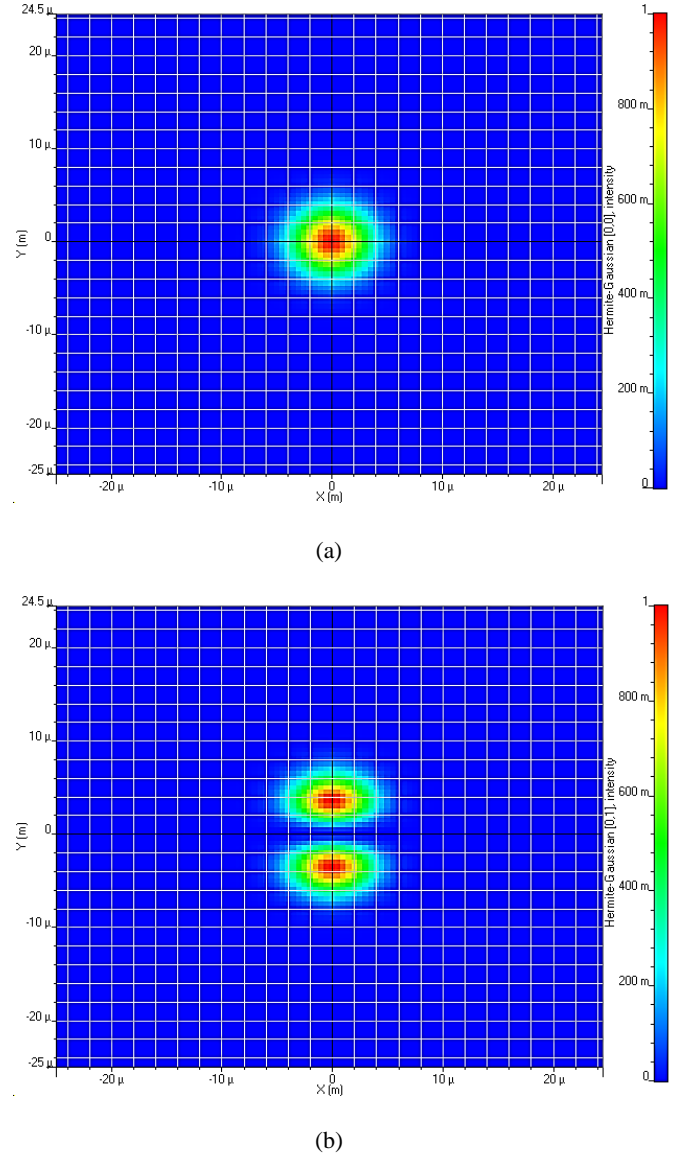

(a)

(b)

Fig. 3. Intensity profiles of excited modes (a) HG00 (b) HG01 (color online)

At the transmitter, 50 Gbit/s 4-level QAM/PSK modulated signal for each channel is OFDM modulated over 512 subcarriers with 1024 IFFT points. A cyclic prefix of 32 value is added to this signal. This signal is further in-phase quadrature modulated at 7.5 GHz by employing a quadrature modulator (QM). The information signal is optically modulated using a distinct HG mode before transmitting over outer space. The received optical power P_R in an IsOWC link is given as [59]:

$$P_R = P_T \eta_T \eta_R \left(\frac{\lambda}{4\pi Z}\right)^2 G_T G_R L_T L_R \quad (4)$$

where P_T represents laser power, η_T and η_R represent optical efficiency of transmitter and receiver respectively, λ represents wavelength, Z represents the transmission range, G_T and G_R represent transmitter and receiver telescopic gain respectively. The transmitter pointing error loss factor L_T depending on transmitter error angle θ_T is given as [59]:

$$L_T = \exp(-G_T\theta_{T^2}) \tag{5}$$

Similarly, receiver pointing error loss factor L_R depending on the receiver error angle θ_R is given as [59]:

$$L_R = \exp(-G_R\theta_{R^2}) \tag{6}$$

Table 1 illustrates the IsOWC link parameters.

Table 1. Link parameters [8, 19, 59]

| Parameter	Value
Operating wavelength	850 nm and 1550 nm
Laser power	30 dBm
Local oscillator power	11 dBm
Laser line width	0.1 MHz
Bit rate/channel	50 Gbit/s
Transmitter/Receiver aperture diameter	150 mm
Transmitter/Receiver optical efficiency	0.8
Space attenuation	0 dB/km
Transmitter pointing error angle	1.1 $urad$
Receiver pointing error angle	1.1 $urad$
Sequence length	65536
Sample per bit	4
Optical amplifier gain	12 dB
Optical amplifier noise figure	4 dB
Photodiode responsivity	1 A/W
Thermal power density	1 e-022 W/Hz
Ionization current	0.9 A
LPF cut off frequency	0.75 × bit rate/8
Additional Loss (pointing losses, synchronization losses, etc.)	5 dB
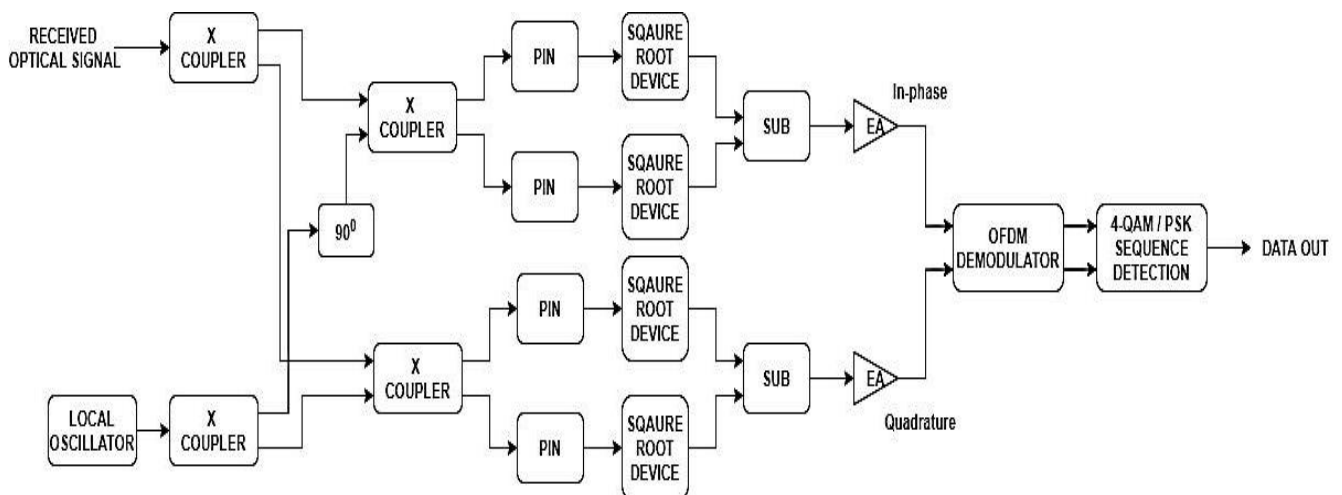
Fig. 4. Schematic of the proposed detection technique

After propagating the outer space, HG00 and HG01 mode are separated at the receiver using a mode filter. Coherent detection is employed for converting the optical beam to electrical signal. An OFDM demodulator and a QM demodulator demodulates the signal and the message bits are retrieved using a 4-QAM/PSK sequence detector. Fig. 4 shows the schematic of the proposed square root device-based enhanced coherent detection. The received

optical information signal is mixed with the corresponding signal from the local oscillator. A 90^0 phase shift is given to separate in-phase and quadrature components. Homodyne balanced detection is performed to convert the optical signal into electrical domain. The balanced detector consists of 2 PIN photodiodes. The information signal while propagating the outer space gets distorted due to many reasons including background radiations, pointing errors, and system losses. The PIN photodiode at the receiver has a square law transfer function which converts the distortion to a non-linear distortion and degrades the signal quality. To improve the signal quality, we have proposed the use of a square root device after each PIN which compensates for square law transfer function of PIN. Fig. 5 shows the transfer function of the square root device, which can be practically implemented using Schottky diodes [60].
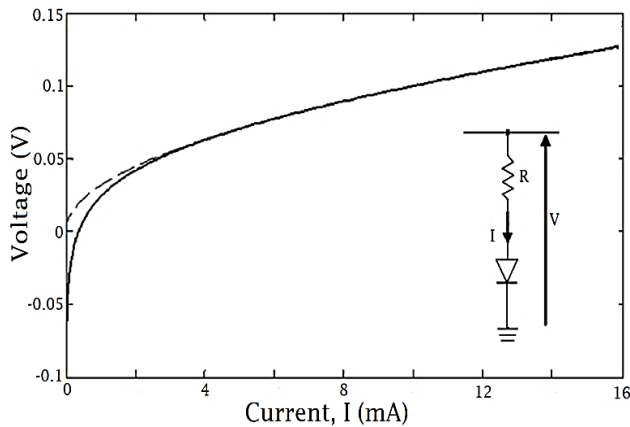

Fig. 5. Square root device transfer function [60]

3. Results and discussions

Fig. 6 reports the BER for 4-PSK and 4-QAM modulation schemes with increasing IsOWC range (850 *nm* operating wavelength is considered). The results demonstrate that with increasing range, the BER increases for both channels in the case of 4-QAM and 4-PSK schemes, as should be expected. Also, channel 1 (HG00 mode) has lower BER then channel 2 (HG01 mode) since the former is more robust to space turbulence. The computed log of BER for 4-PSK modulation is -4.5, -1.45, and -0.70 for HG00 mode and -3.97, -1.07, and -0.57 for HG01 mode at 10000, 35000, and 60000 km respectively. Similarly, the log of BER for 4-QAM modulation is -4.55, -1.60, -0.82 for HG00 mode and -3.6, -1.28, and -0.64 for HG01 mode at 10000, 35000, and 60000 km respectively. For 4-PSK modulation scheme, the achievable range with faithful BER of 3.8×10^{-3} (i.e. FEC Threshold Limit) for both channels is 20000 km. The results presented demonstrate that by using the proposed 4-QAM-based IsOWC link, 20500 km transmission range for both channels is achievable with faithful BER performance. This can be attributed to the fact that in IsOWC link, the

signal attenuation offered by outer space is 0 dB/km. Further, 100 Gbit/s information has been transported over long-range communication using a single wavelength laser beam by incorporating hybrid CO-OFDM-MDM techniques.

Also, the results show that 4-QAM reports better performance than 4-PSK. This is because PSK modulation modulates the information using a single degree of freedom (i.e. phase only) whereas QAM modulation modulates the information using two degrees of freedom (i.e. intensity and phase) which makes it more robust to space turbulence and background noise radiations [61, 62]. The efficiency of the demodulator unit to differentiate distinct information signal vectors under the influence of noise is dependent on the separation between the vector endpoints. This suggests that the performance of the receiver in the presence of noise will enhance by using QAM modulation where the signal vectors differ in both intensity and phase as compared to PSK modulation where signal vectors differ in phase only. Further, for the same order of modulation, QAM modulation has a higher Euclidean distance between the corresponding signal points as compared to PSK modulation [63].
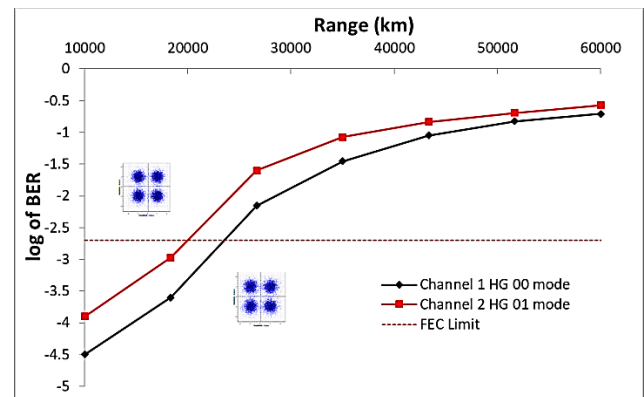

(a)
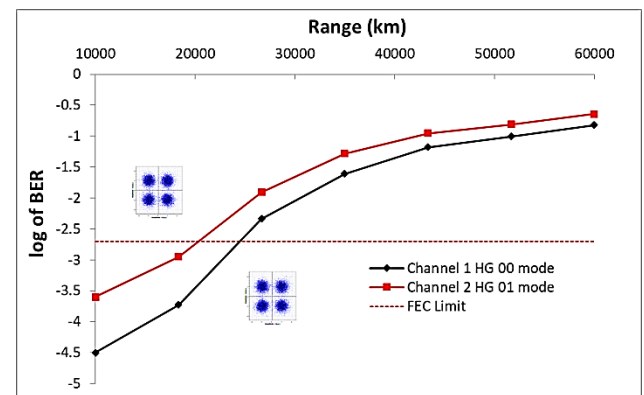
(b)

Fig. 6. Log of BER v/s IsOWC range using (a) 4-PSK (b) 4-QAM modulation (color online)

Fig. 7 compares the performance of 850 nm and 1550 nm operating wavelengths on the proposed 100 Gbit/s CO-OFDM-MDM-based IsOWC link performance using 4-QAM modulation. The results show that for channel 1 (HG00 mode), the maximum achievable transmission range is 24500 km for 850 nm operating wavelength and 13000 km for 1550 nm operating wavelength. Similarly, for channel 2 (HG01 mode), the maximum achievable transmission range is 20500 km for 850 nm operating wavelength which reduces to 11500 km for 1550 nm operating wavelength. 850 nm operating wavelength shows a better performance for realizing long-haul high-speed IsOWC links.
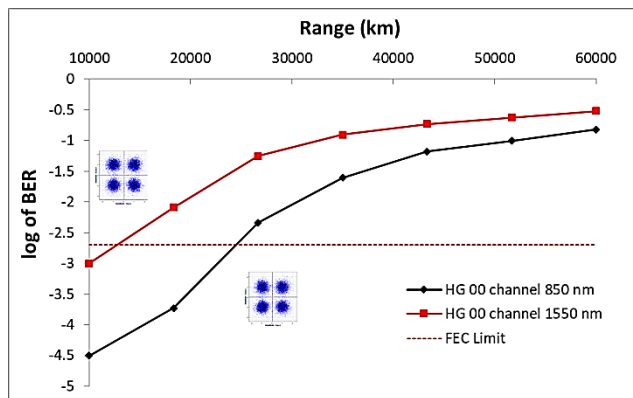

(a)
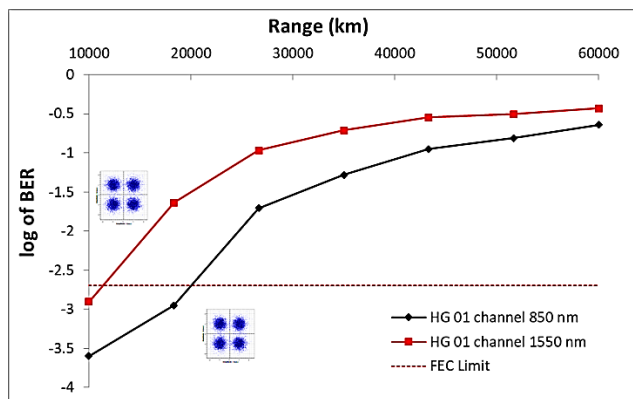
(b)

Fig. 7. Log of BER v/s IsOWC range for (a) channel 1 (HG00 mode) (b) channel 2 (HG01 mode) using different operating wavelengths (color online)

Fig. 8 (a) and (b) reports the BER performance of the link with increasing receiver pointing errors and transmitter pointing errors respectively at 10000 km IsOWC range (850 nm wavelength and 4-QAM modulation is considered). As seen from Fig. 8, increasing pointing errors increases the BER of the system. Channel 1 (HG00 mode) has an acceptable BER up to receiver and transmitter pointing error angle of 2.7 μrad whereas

channel 2 (HG01 mode) has an acceptable BER up to receiver and transmitter pointing error angle of 2.4 μrad.
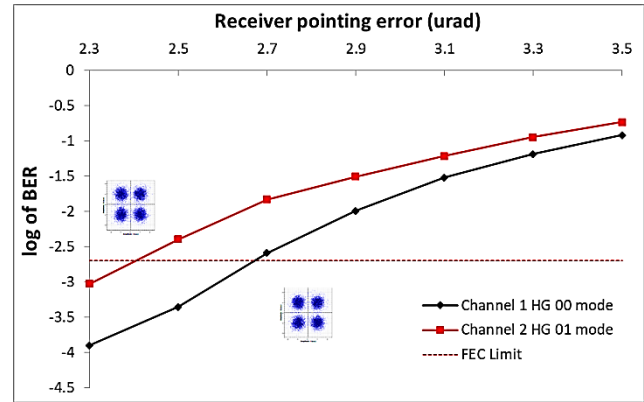
(a)
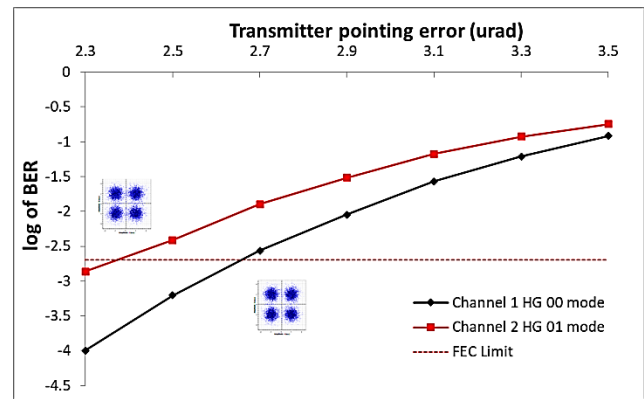
(b)

Fig. 8. Log of BER of the received signal with increasing (a) receiver pointing error (b) transmitter pointing error (color online)

The information bearing laser beam propagating the outer space suffers from linear distortion due to path loss, pointing errors, and background noise radiations. The PIN photodiodes used at the receiver terminal have square law transfer characteristics which convert the linear distortion of the information signal to non-linear distortion, further deteriorating the signal quality. In order to compensate for the non-linear response of the PIN photodiode and improve the link performance, we propose a square root device after each PIN to compensate for its square law transfer characteristics. Fig. 9 illustrates the performance improvement of link under increasing receiver pointing errors at 10000 km IsOWC range using the proposed detection. It can be seen that by incorporating the proposed square root device, the link transmits 100 Gbit/s successfully at 10000 km up to a receiver pointing error of 4.3 μrad as compared to 2.7 μrad without using the square root device.
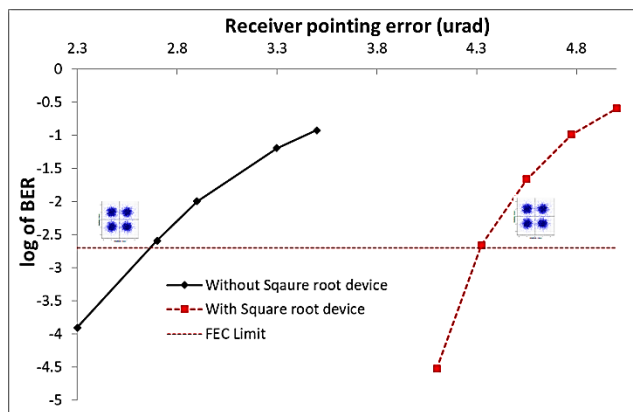
Fig. 9. Improved performance investigation of the IsOWC link using the proposed square root device (color online)

Fig. 10 reports the decomposition of distinct spatial channels into linear polarized (LP) modes at the receiver terminal. For channel 1 (HG00 mode), 87.26% of the signal power is coupled to LP01 mode and the remainder is transferred to the adjacent modes. Similarly for channel 2 (HG01 mode), 68.17% of the signal power is coupled to LP11 mode. Higher intermodal power coupling is observed for HG01 mode, which justifies the results of the link performance in Figs. 6-8.
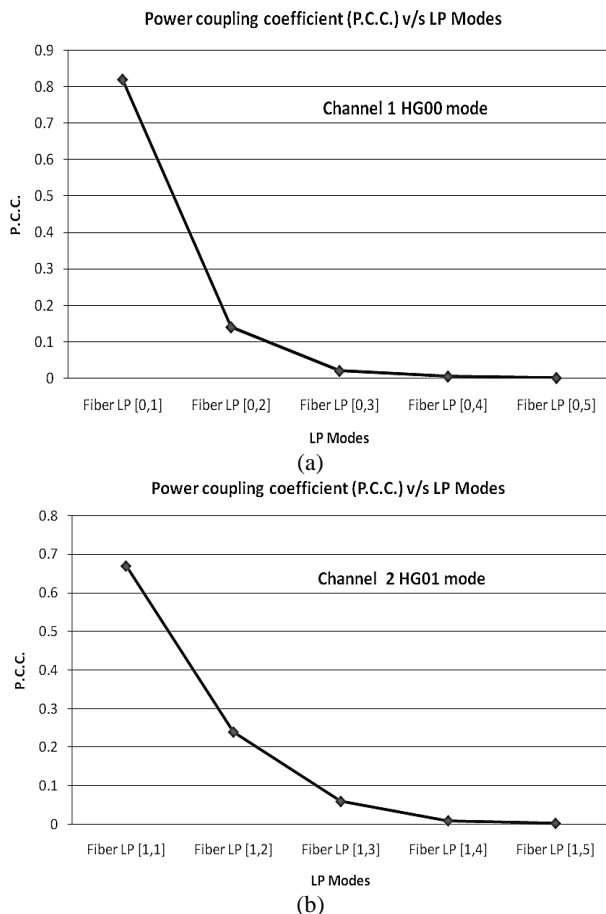

(a)

(b)

Fig. 10. Modal decomposition analysis

4. Conclusion

In this work, a long-haul high data rate cost-effective IsOWC system employing hybrid CO-OFDM and MDM techniques is proposed. The results show that 4-QAM scheme demonstrates lower BER and thus performs better as compared to 4-PSK scheme and 850 nm is a better candidate for operating wavelength. Through numerical simulations, we report faithful 100 Gbit/s transportation at 20500 km using 4-QAM modulation and 850 nm operating wavelength. Further, it can be concluded that 10000 km transmission is achievable up to transmitter and receiving pointing error angle of 2.4 μrad. Also, we propose a square root device-based enhanced detection to improve the link performance. The IsOWC link using the proposed detection demonstrates good BER performance up to 4.3 μrad pointing error angle which shows considerable improvement in the link performance. In future works, the proposed IsOWC link needs to be practically realized by doing real time experiments. Also, higher data transmission rates can be achieved by using more spatial channels.

References

[1] M. Singh, J. Malhotra, Wireless Pers. Commun. **107**, 1 (2019).
[2] H. Kaushal, G. Kaddoum, IEEE Communications Surveys & Tutorials **19**, 57 (2017).
[3] T. Nielsen, G. Oppenhauser, Proc. SPIE, Free Space Laser Comm. Tech. XIV **4635**, 1 (2002).
[4] Vishal Sharma, Naresh Kumar, Optik **286**, 99 (2013).
[5] Q. Wang, T. Song, M.-W. Wu, T. Ohtsuki, M. Gurusamy, P.-Y. Kam, OptoElectronics and Communications Conference (OECC) Held Jointly with 2016 International Conference on Photonics in Switching (PS), 21st, 1 (2016).
[6] M. Singh, Journal of Optical Communications **39**(1), 49 (2016).
[7] G. A. Koepf, R. G. Marshalek, D. L. Begley, AEU-International Journal of Electronics and Communications **56**(4), 232 (2002).
[8] B. Patnaik, P. K. Sahu, IET Communications **6**(16), 2561 (2012).
[9] G. Kumari, C. Selwal, Proc. of International Conference on Recent Advances and Innovations in Engineering (ICRAIE), Jaipur, pp. 1-5 (2016).
[10] T. Song, Q. Wang, M.-W. Wu, P.-Y. Kam, Opt. Express **24**, 11950 (2016).
[11] A. Alipour, A. Mir, A. Sheikhi, Optik **127**(19), 8135 (2016).
[12] R. Kaur, H. Kaur, Optik **128**, 755 (2018).
[13] S. Kumar, S. Gill, K. Singh, Wireless Personal Communications **98**(1), 1461 (2018).
[14] S. Chaudhary, A. Sharma, V. Singh, Optik **176**, 185 (2019).
[15] D. Amanor, W. Edmonson, F. Afghah, IEEE Transactions on Aerospace and Electronic Systems **54**(6), 2888 (2018).

[16] J. Padhy, B. Patnaik, Proc. of IEEE 5th International conference on emerging technologies and applied sciences, Bangkok, Thailand 1 (2018).

[17] Naresh Kumar, Optik **125**(8), 1945 (2014).

[18] Pooja Gopal, V. K. Jain, Subrat Kar, Proc. SPIE 9248, Unmanned/Unattended Sensors and Sensor Networks **X**, 92480V (2014).

[19] J. Padhy, B. Patnaik, Optical and Quantum Electronics **51**, 213 (2019).

[20] Kang Zong, Jiang Zhu, Da Ku, Proc. of 15th International Conference on Optical Communications and Networks (ICOCN), Hangzhou **2016**, 1 (2016).

[21] S. Pradhan, P. K. Sahu, R. K. Giri, B. Patnaik, Proc. of International Conference on Microwave, Optical and Communication Engineering (ICMOCE), Bhubaneswar **2015**, 250 (2015).

[22] Kang Zong, Appl. Opt. **57**, 9464 (2018).

[23] A. N. Z. Rashid, M. Tabbour, K. Natarajan, International Journal of Satellite Communications and Networking **38**(1), 31 (2019).

[24] S. Chaudhary, X. Tang, A. Sharma, B. Lin, X. Wei, A. Parmar, Optical and Quantum Electronics. **51**, 148 (2019).

[25] W. Shieh, H. Bao, Y. Tang, Opt. Express **16**(2), 841 (2008).

[26] A. J. Lowery, J. Armstrong, Opt. Express **14**, 2079 (2006).

[27] X. Liu, F. Buchali, R. W. Tkach, J. Lightwave Technol. **27**(16), 3632 (2009).

[28] S. Chandrasekhar, X. Liu, B. Zhu, D. W. Peckham, Proceedings of European Conference on Optical Communications, paper PD 2.6 (2009).

[29] A. Lowery, J. Armstrong, Opt. Express **14**(6), 2079 (2006).

[30] G. Bosco, A. Carena, V. Curri, P. Poggiolini, F. Forghieri, IEEE Photonics Technol. Lett. **22**(15), 1129 (2010).

[31] S. Chaudhary, A. Sharma, N. Chaudhary, Journal of Optical Communications **37**(4), 375 (2016).

[32] S. Chaudhary, R. Kapoor, A. Sharma, Journal of Optical Communications **40**(2), 143 (2017).

[33] S. Chaudhary, N. Chaudhary, S. Sharma et al., Journal of Optical Communications **39**(1), 87 (2016).

[34] M. Singh, N. Singh, Journal of Optical Communications **39**(2), 137 (2016).

[35] N. Badar, R. Jha, I. Towfeeq, Optical and Quantum Electronics **50**, 1 (2018).

[36] Mehtab Singh, Jyoteesh Malhotra, Wireless Personal Communications **107**, 1549 (2019).

[37] Mehtab Singh, Jyoteesh Malhotra Optical Engineering **58**(4), 046112 (2019).

[38] Rajan Gupta, R. S. Kaler, Optical Engineering **55**(5), 056102 (2016).

[39] Yi-Li Chung et al., Laser Physics Letters **13**(7), 1 (2016).

[40] Rajan Gupta, R. S. Kaler, Optelectron. Adv. Mat. **11**(11-12), 643 (2017).

[41] Rajan Gupta, R. S. Kaler, Optelectron. Adv. Mat. **12**(7-8), 441 (2018).

[42] Y. Fazea, Optik **183**, 994 (2019).

[43] B. J. C. Schmidt, A. J. Lowery, J. Armstrong, J. Lightw. Technol. **26**(1), 196 (2008).

[44] W. Shieh, C. Athaudage, Electron. Lett. **42**, 587 (2006).

[45] S. L. Jansen, I. Morita, N. Takeda, H. Tanaka, Proc. OFC/NFOEC 2007, Anaheim, CA, Paper PDP15 (2007).

[46] S. L. Jansen, I. Morita, T. C. W. Schenk, N. Takeda, H. Tanaka, J. Lightw. Technol. **26**, 6 (2008).

[47] A. J. Lowery, J. Armstrong, Opt. Express **13**, 10003 (2005).

[48] J. M. Tang, P. M. Lane, K. A. Shore, IEEE Photon. Technol. Lett. **18**, 205 (2006).

[49] S. C. J. Lee, F. Breyer, S. Randel, M. Schuster, J. Zeng, F. Huiskens, H. P. A. van den Boom, A. M. J. Koonen, N. Hanik, Proc. OFC/NFOEC 2007, Anaheim, CA, Paper PDP6 (2007).

[50] S. C. J. Lee, F. Breyer, S. Randel, O. Ziemann, H. P. A. van den Boom, A. M. J. Koonen, Proc. OFC/NFOEC 2008, San Diego, CA, Paper, OWB3 (2008).

[51] O. Gonzalez, R. Perez-Jimenez, S. Rodriguez, J. Rabadan, A. Ayala, IEE Proc. Optoelectron. **153**, 139 (2006).

[52] J. Armstrong, Journal of Lightwave Technology **27**(3), 189 (2009).

[53] A. Ghatak, K. Thyagarajan, Introduction to Fiber Optics, Cambridge (1998).

[54] Jose A Rodrigo, Tatiana Alieva, Maria L Calvo, Opt. Express **15**(5), 2190 (2007).

[55] E. G. Abramochkin, V. G. Volostnikov, J. Opt. A: Pure Appl. Opt. **6**(5), S157 (2004).

[56] E Abramochkin, V. Volostnikov, Opt. Commun. **83**(1-2), 123 (1991).

[57] Martin J. Baastians, Tatiana Alieva, Journal of Physics A **38**(6), L73 (2005).

[58] Yi Wang, Yujie Chen, Yanfeng Zhang, Hui Chen, Siyuan Yu, Journal of Optics **18**, 055001 (2015).

[59] Q. Tan, W. Chen, Proc. PIERS, Hangzhou, China 1394 (2018).

[60] J. Prat, A. Napoli, J. M. Gene, M. Omella, P. Poggiolini, V. Curri, Proceedings of the ECOC 2005, Glasgow, UK, 106 (2005).

[61] J. M. Kahn, Optical Amplifiers and Their Applications/Coherent Optical Technologies and Applications, Technical Digest (CD) (Optical Society of America), paper CThC1 (2006).

[62] J. M. Kahn, K. P. Ho, Forestieri E. (eds), Optical Communication Theory and Techniques, Springer, Boston, MA (2005).

[63] P. Krishnan, U. Jana, B. Kanekal Ashokkumar, IET Communications **12**(16), 2046 (2018).

_____
*Corresponding author: mehtab91singh@gmail.com